



**HAL**  
open science

# Harnessing Catalysis Selectivity and Isophorone Diisocyanate Asymmetry for Tailored Polyurethane Prepolymers and Networks

Priscilla Arnould, Frédéric Simon, Stéphane Fouquay, Francis Pardal, Guillaume Michaud, David Gajan, Jean Raynaud, Vincent Monteil

► **To cite this version:**

Priscilla Arnould, Frédéric Simon, Stéphane Fouquay, Francis Pardal, Guillaume Michaud, et al.. Harnessing Catalysis Selectivity and Isophorone Diisocyanate Asymmetry for Tailored Polyurethane Prepolymers and Networks. *Macromolecules*, 2022, 55 (8), pp.3344-3352. 10.1021/acs.macromol.1c02491 . hal-03728235

**HAL Id: hal-03728235**

**<https://hal.science/hal-03728235>**

Submitted on 20 Jul 2022

**HAL** is a multi-disciplinary open access archive for the deposit and dissemination of scientific research documents, whether they are published or not. The documents may come from teaching and research institutions in France or abroad, or from public or private research centers.

L'archive ouverte pluridisciplinaire **HAL**, est destinée au dépôt et à la diffusion de documents scientifiques de niveau recherche, publiés ou non, émanant des établissements d'enseignement et de recherche français ou étrangers, des laboratoires publics ou privés.

# Harnessing catalysis selectivity and isophorone diisocyanate asymmetry for tailored polyurethane prepolymers and networks

Priscilla Arnould<sup>†,‡</sup>, Frédéric Simon<sup>‡</sup>, Stéphane Fouquay<sup>‡</sup>, Francis Pardal<sup>‡</sup>, Guillaume Michaud<sup>‡</sup>,  
David Gajan<sup>§</sup>, Jean Raynaud<sup>†\*</sup>, Vincent Monteil<sup>†\*</sup>

<sup>†</sup> Université de Lyon, Université Lyon 1, CPE Lyon, CNRS, UMR 5128, Laboratoire CP2M, Equipe PCM, 69616 Villeurbanne  
– France

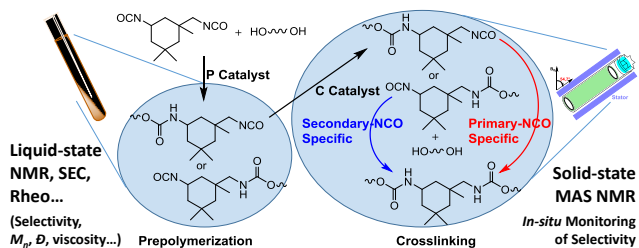
<sup>‡</sup> Bostik Smart Technology Center, ZAC du bois de Plaisance, 60280 Venette – France

<sup>§</sup> Université de Lyon, Centre de RMN à Très Hauts Champs de Lyon, UMR5082, CNRS/ENS de Lyon/UCB Lyon, 69100  
Villeurbanne – France

\* [jean.raynaud@univ-lyon1.fr](mailto:jean.raynaud@univ-lyon1.fr); [vincent.monteil@univ-lyon1.fr](mailto:vincent.monteil@univ-lyon1.fr)

**KEYWORDS.** *NCO-terminated prepolymers, Crosslinked polyurethanes, Metallic catalysts, Organocatalysts, Solid-state NMR*

For Table of contents use only



We synthesized IPDI-based polyurethane materials via a typical industrial two-stage process: 1) synthesis of NCO-terminated prepolymers & 2) crosslinking with polyols. Using multiple macroscopic (SEC, rheometry, DSC, DMA) & spectroscopic techniques (liquid- and solid-state NMR & FTIR), we evidenced that through appropriate choice of catalyst combinations, we could tune the mechanical PU properties through selective urethane bond formation either from primary or secondary NCO moieties of IPDI - 1) at the prepolymerization stage; and corresponding prepolymers - 2) at the crosslinking stage.

---

**ABSTRACT:** We synthesized polyurethane materials *via* a typical industrial two-stage process based on the synthesis of NCO-terminated prepolymers followed by their crosslinking with polyols. We investigated the influence of metallic and organic catalysts on i) polyaddition kinetics between a challenging monomer (the aliphatic and asymmetric isophorone diisocyanate *a.k.a.* IPDI) and polyols, and on ii) the structure and properties of corresponding polyurethane prepolymers and networks. Tin-free catalysts (Ti, Zn-based) and even metal-free catalysts (guanidines, amidines, amines) are competitive alternatives to a standard tin catalyst. Beside the activity criterion, appropriately choosing the catalyst allows to adjust the prepolymer structure relying on respective selectivities toward primary vs. secondary isocyanate moieties, as well as propensity to favor functionalization over chain extension. By quantitative NMR spectroscopy, three different catalyst selectivities are pinpointed, which either favor the primary or the secondary isocyanate functions or promote their isoreactivity. These selectivities are harnessed both at the prepolymerization and crosslinking stages to significantly decrease reaction time by judicious and innovative combinations of catalysts with opposite selectivities toward primary/secondary isocyanates. We eventually evidenced the efficiency of this methodology for tailored polyurethane-based materials through *in-situ* solid-state NMR monitoring of the crosslinking stage.

---

## INTRODUCTION

Polyurethanes are an essential class of polymers due to their versatility and unique intrinsic properties, brought about by the tailored double network of covalent and H-bonding crosslinks, advantageous in various applications such as paintings, foams (CO<sub>2</sub> as porogen), adhesives and mastics.<sup>1-5</sup> Discovered by Otto Bayer, polyurethanes result from polyaddition reactions between polyisocyanate and polyols, with functionalities usually ranging from 2 to 3.<sup>1-4</sup> For reactivity (enhanced kinetics) and selectivity reasons, polyurethanes are essentially obtained from aromatic diisocyanates such as 4,4'-methylenebis-(phenylisocyanate) (4,4'-MDI) and tolylene diisocyanate (2,4-TDI) and polyols in presence of tin-based catalysts.<sup>1-4,6</sup> Nevertheless, research efforts have been made in order to decrease overall polyurethanes' toxicity by using more ecofriendly diisocyanate monomers and catalysts. Underexploited industrially due to their intrinsically lower reactivities (and higher prices), symmetric and asymmetric aliphatic diisocyanates, such as hexamethylene diisocyanate (HDI) and isophorone diisocyanate (IPDI), could nonetheless be effective alternatives to aromatic diisocyanates, and even become competitive with appropriate catalysis, preferentially tin-free.<sup>1-4,6,7</sup> Both existing and new material properties could for instance be targeted for aliphatic-based polyurethanes. To this end, more ecofriendly catalysts have been stud-

ied to replace standard tin catalysts with either metallic catalysts based on sustainable metals such as titanium, iron, copper and zinc, or organocatalysts such as nitrogen-centered Lewis bases (amines, guanidines and amidines...)<sup>8-16</sup>

Among aliphatic diisocyanate monomers, isophorone diisocyanate (IPDI) is the most promising candidate since the volatility of HDI precludes its widespread use. IPDI is an asymmetrical diisocyanate, owning a primary aliphatic and a secondary cycloaliphatic isocyanate functions with two uneven intrinsic reactivities.<sup>17-20</sup> Research evidenced the secondary isocyanate group as the more reactive due to a lower steric hindrance in chair conformation compared to the primary isocyanate function.<sup>17-20</sup> Only few articles studied the influence of catalysts on polyurethanes kinetics but also on the primary and secondary isocyanate reactivities and consequently on the structure/properties of resulting polyurethanes.<sup>9,11,17-27</sup> In this literature, it was identified that the majority of catalysts enhanced the reaction of the secondary isocyanate function of IPDI with an incoming alcohol moiety compared to the primary isocyanate.<sup>8,19,26</sup> However, some articles highlighted different catalyst behaviors and reactivities toward these two isocyanates groups.<sup>9,19,22,23,26,28,29</sup> In fact, the organic catalyst 1,4-diazabicyclo(2.2.2)octane (DABCO) slightly favored the reactivity of the primary isocyanate function of IPDI or led to the isoreactivity of both isocyanates.<sup>19,22,23,26</sup> Triethylamine, 7-methyl-1,5,7-triazabicyclo(4.4.0)dec-5-ene (MTBD) or even metallic catalysts based on metals such as zirconium seemed to promote the equireactivity of both isocyanate functions.<sup>8,11,30</sup> However, the study of the primary vs. secondary selectivities of catalysts are limited to a few catalysts and are mainly realized through model reactions with monoalcohol, often non-representative of an actual polyurethane synthesis. Moreover, these selectivities are under-exploited since they could have, if synergized, considerably decreased prepolymerization as well as crosslinking reaction times and few articles tended to rationalize the mechanisms involved during polyurethane synthesis. To this purpose, in the present work, crosslinked polyurethane-based materials are synthesized *via* a two-step process in presence of a wide variety of catalysts (Figures 1 and 2).

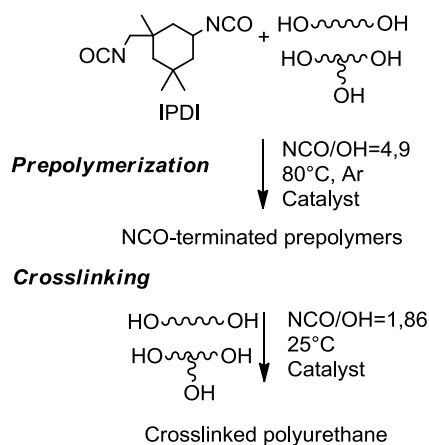
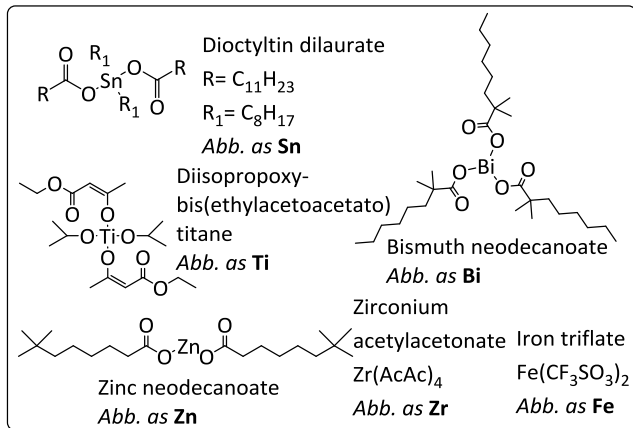


FIGURE 1. Synthesis of crosslinked polyurethane *via* a two-step process.

At the prepolymerization stage, NCO-terminated prepolymers were synthesized in bulk with isophorone diisocyanate and two poly(propylene glycol)-based diol and triol (PPG) (secondary alcohol functions, global functionality of polyol blend was equal to 2.37, characteristics are given in SI). Crosslinking of these prepolymers then takes place with polyester-based diol (primary alcohol functions), polyether-based triol (secondary alcohol functions) and adventitious air moisture (Materials and Methods, SI). This example is representative of a polyurethane-based adhesive coating. Obviously the methodology could be implemented on other formulations and corresponding applications. If so the quantitative values (or even the overall catalytic effect) might differ (ex: variation of the diols).

Prepolymerization and crosslinking catalysts are selected among metallic and organic catalysts to identify their impact on kinetics, on the primary and secondary isocyanate-biased reactivities but also on the structure/properties of obtained polyurethanes. In this work, three catalysts behaviors are evidenced, in particular regarding their mode of activation of primary vs. secondary isocyanates, harnessing NMR spectroscopy. By further using spectroscopic techniques, namely FTIR and solid-state NMR, tin or even metal-free prepolymerization and crosslinking catalyst combinations with opposite selectivities have been identified to optimize kinetics and prepolymer/network properties. The successive reaction of primary and secondary isocyanate groups of IPDI at the two stages, induced by appropriate choice of combined catalysts, is a powerful strategy that can be implemented to synthesize tailored polyurethane-based architectures.

### Metallic catalysts



### Organic catalysts

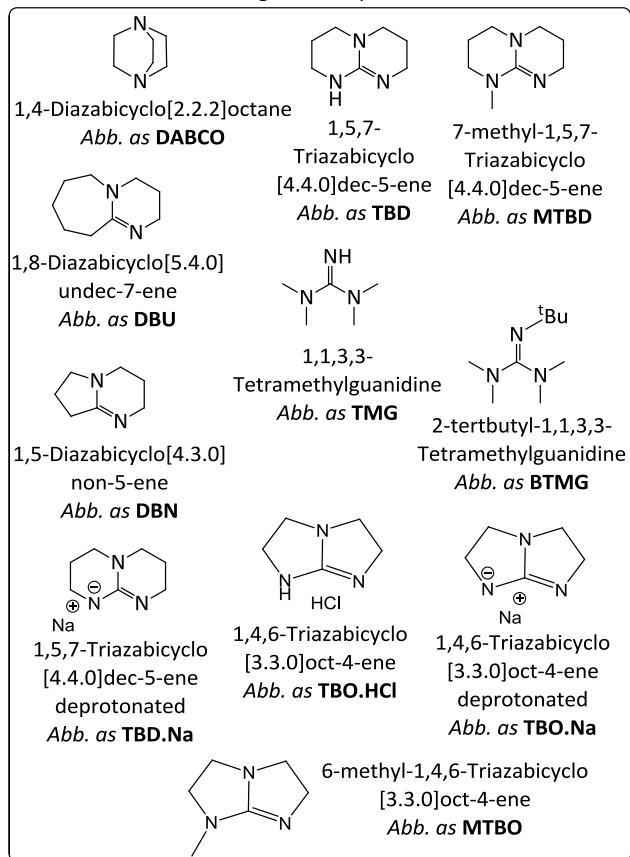


FIGURE 2. Structure of the selected catalysts and their abbreviation employed in this work.

## RESULTS AND DISCUSSION

Kinetics of NCO-terminated polyurethane prepolymers syntheses - Prepolymerization stage.

NCO-terminated polyurethane prepolymers are obtained from polyaddition reactions between IPDI and two poly(propylene glycol)-based diol and triol (PPG) under argon at a NCO/OH ratio equal to 4.9 and at 80°C. This high

ratio is typical of PU coatings for laminating/adhesive applications, and the associated reactivity bias should also emerge from the high concentration of NCO in the medium. At this stage, minimizing the water content yielding urea side-products rather than urethane desired moieties is essential to the control of viscosity (necessarily low for ease-of-coating purposes). To determine the impact of catalysts over prepolymerization kinetics, tin-free or even metal-free catalysts were used among metallic (Ti, Zn, Bi, Zr, Fe) and organic catalysts (amine, guanidine, amidine) (Figure 2).

To unveil the relative efficiency of each catalyst, different molar amounts of metallic and organic catalysts are selected in order to match similar kinetics and prepolymerization time as tin catalysts (**Sn**), which is the reference in the polyurethane field. Each catalyst amount is thus compared to the amount of tin catalysts necessary to provide comparable kinetics and suggest competent alternative to tin catalyst. By using FTIR-ATR analysis in order to compare these catalyst activities, the reaction progress is determined by monitoring the isocyanate consumption, which is directly correlated to the decrease of the NCO stretching band at  $2251\text{ cm}^{-1}$  (Figure S1, SI). The homogeneity of the sample during the prepolymerization (lower-than-ambient- $T_g$  prepolymer) provided quasi-quantitative FTIR analysis and allowed for the comparison of the different catalyzed and uncatalyzed prepolymerizations. At a NCO/OH ratio of 4.9, the maximum conversion value of NCO functions is equal to 20.4%. For uncatalyzed system, the reaction between IPDI with polyether-based diol and triol is noticeably slow due to the low reactivity of the aliphatic isocyanate IPDI and 42 hours were required to obtain the final NCO-terminated prepolymer (constant NCO stretching band determined by FTIR spectroscopy). Under these conditions, the use of catalysis is mandatory to significantly decrease the reaction time, and unlock industrial applications.

Metallic catalysts were mostly found to have an important catalytic activity and reduced the reaction time in a range of 30 minutes to 4 hours depending on catalyst and molar amounts on a par with standard tin catalyst, comprised from 1 to 10 times the reference (Figure 3, Table 1). We acknowledge the unusual comparison with these different molarities, however for industrial purposes the exact amounts tend to matter less than achieving comparable kinetics, factoring in a balance price/benefits of selected catalysis.



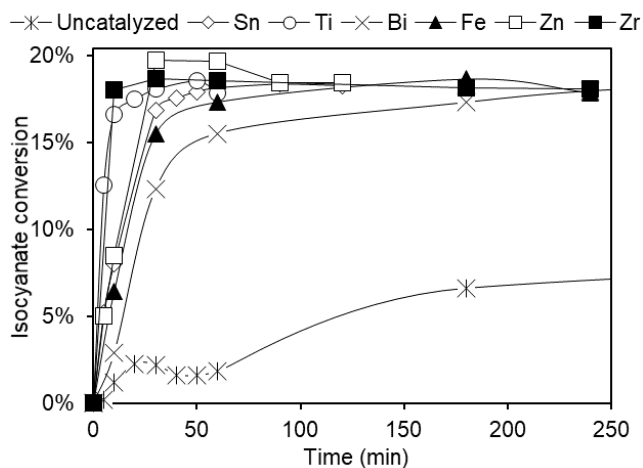


FIGURE 3. Influence of metallic catalysts on the kinetics of the prepolymerization reaction at 80°C determined by FTIR-ATR.

TABLE 1. Effects of catalysts on reaction times for the synthesis of NCO-terminated prepolymers at 80°C and NCO/OH ratio equal to 4.9.

Catalyst (ppm)	Molar amount of catalysts compared to tin catalyst (~Sn 60 ppm)	Approximative time of reaction (min) <sup>a</sup>
Uncatalysed	0	2520
Zr 390ppm	10	30
Ti 70ppm	2	60
Co 42ppm	2	60
Sn 60ppm ( <i>ref</i> )	1	90
Zn 240ppm	7	90
Fe 240ppm	8	180
Bi 58ppm	1	240-300
TBD.Na 375ppm	40	120

<b>MTBO 392ppm</b>	40	120
<b>TBO.Na 442ppm</b>	40	135
<b>MTBD 480ppm</b>	40	180
<b>BTMG 3500ppm</b>	250	180
<b>TMG 2300ppm</b>	250	240
<b>DBU 600ppm</b>	50	>360
<b>DABCO 450ppm</b>	50	>480
<b>DBN 495ppm</b>	50	1740
<b>TBD 440ppm</b>	40	1680
<b>TBO.HCl</b>		
<b>462ppm</b>	40	1560

a. Time to reach a constant value of the absorption of the stretching band of NCO determined by FTIR.

As for organic catalysts, only bicyclic and acyclic guanidines **MTBD**, **TMG** and **BTMG** are efficient under these conditions, and significantly reduced the reaction time to 3 hours compared to the 42 hours for the uncatalyzed system (Figure 4, Tableau 1), albeit using substantially higher catalytic amounts.

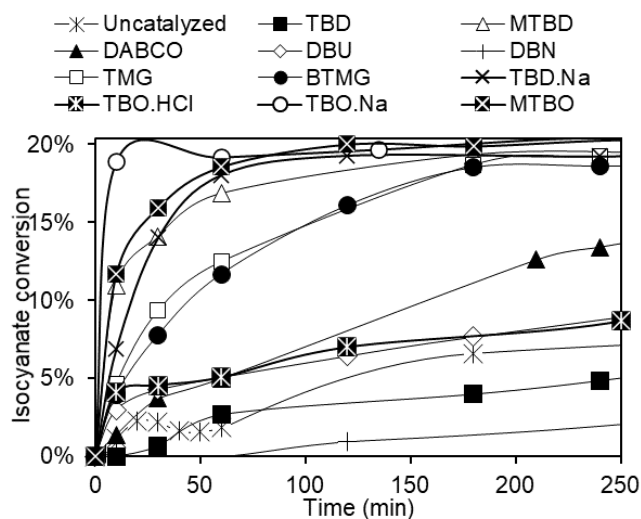


FIGURE 4. Influence of organic catalysts on the kinetics of the prepolymerization reaction at 80°C determined by FTIR-ATR.

On the other hand, organic catalysts such as amine (**DABCO**), amidine (**DBN**, **DBU**) and the guanidine **TBD** presented low catalytic activities under these conditions and required more than 6 hours to obtain the final NCO-terminated prepolymer (constant NCO band area determined by FTIR). It is important to notice again that efficient organic catalysts **MTBD**, **TMG** and **BTMG** were less effective than tin and even metallic catalysts because their molar amount are multiplied by 40 or 250 compared to the needed molar amount of tin catalysts to achieve comparable effectiveness (Table 1). This emphasizes the influence of catalysts on prepolymerization rates and suggest different metallic and organic catalysts as interesting alternatives to tin catalysts, if mandated by the application, either being food- or skin-contact. Landais *et al.* suggested that the low catalytic activities of amidines **DBU** and **DBN** result from the formation of irreversible adducts between these catalysts and two molecule of isocyanate monomer (see Figure S2 for a generalized mechanism, SI).<sup>11</sup> They used benzyl isocyanate as a model compound.<sup>11</sup> In the case of the guanidine **TBD**, which possesses a chemical structure akin to the efficient catalyst **MTBD**, this low activity is explained by the high stability of the urea intermediate species obtained from the reaction of **TBD** with isocyanate (Figure S3, SI).<sup>11,31</sup> The influence of the cycle tension and the nature of the group carried by the nitrogen in  $\beta$ -position of the C=N double bond has also been studied thanks to the successful synthesis of different organic catalysts (Table 1, Figures S4, S5 and S6 in SI, detailed of the catalysts syntheses are provided in SI). The significant reactivity of the deprotonated catalysts or bearing a methyl group derived from **TBD** and **TBO** (**TBD.Na**, **MTBD**, **TBO.Na**, **MTBO**) exposed that the hydrogen carried by the nitrogen is responsible for the low activity of these catalysts during the prepolymerization. The deprotonation or the presence of methyl group could either decrease the stability of the urea intermediate species from the reaction of these catalysts with isocyanate or even preclude its formation, and explain the high activity of these catalysts. Analytical techniques such as SEC-THF and rheometry highlighted that NCO-terminated prepolymers structure and properties (molar masses, viscosity) are almost independent of the choice of catalysts (Table S1, SI), which is not surprising at this biased NCO/OH ratio, aimed at maximizing functionalization over chain-extension to limit prepolymers' viscosity for easy coating of prepolymers during crosslinking.

Selectivity of catalysts toward the primary and secondary isocyanate functions of IPDI - Prepolymerization stage.

IPDI is an aliphatic diisocyanate monomer featuring a primary and a secondary isocyanate functions with different reactivities. The secondary isocyanate function is identified as intrinsically the more reactive function.<sup>17-20</sup>

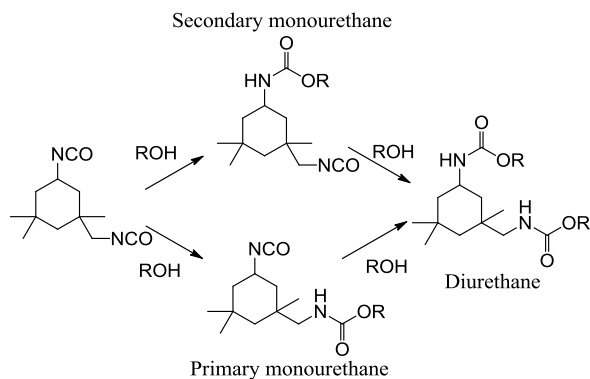


FIGURE 5. NCO-terminated prepolymers structures depending on the primary and secondary isocyanate functions reactivity.

At high ratio NCO/OH (equal to 4.9), this asymmetry leads to the synthesis of different NCO-terminated prepolymers structures among which diurethane, primary or secondary monourethane are commonly obtained (Figure 5).

Liquid NMR analyses on NCO-terminated prepolymers were realized to determine the selectivity of catalysts toward these two isocyanate functions (Figures S7 and S8, SI). Two different carbonyl C=O(urethane) signals are identified by  $^{13}\text{C}$  NMR in acetone- $d_6$  and differentiated the urethane moieties resulting from the reaction of either the primary or the secondary isocyanate functions with the alcohol groups (Figure 6 and Figure S8 SI).

These analyses were considered quasi-quantitative due to the same nature of C=O bond promoting similar relaxation times for  $^{13}\text{C}$  nuclei, the high concentration of prepolymers used and the adjustment of the delay time  $d_1$  (experiment details are provided in SI). However, NMR analyses did not allow to distinguish the urethane function of monourethane-featuring from that of diurethane-featuring prepolymers (see Figure 5). We assumed that the contribution of C=O(diurethane) in each carbonyl signal is comparable in first approximation, with again the bias toward functionalization over chain-extension. Consequently, the ratio of the integration of the two carbonyl signals, i.e.  $S = (\text{C=O(primary monourethane)})/(\text{C=O(secondary monourethane)})$  is directly related to the difference in reactivity of isocyanate functions and to the selectivity of the catalyst towards said functions ( $S$ , calculated thanks to liquid NMR analysis).

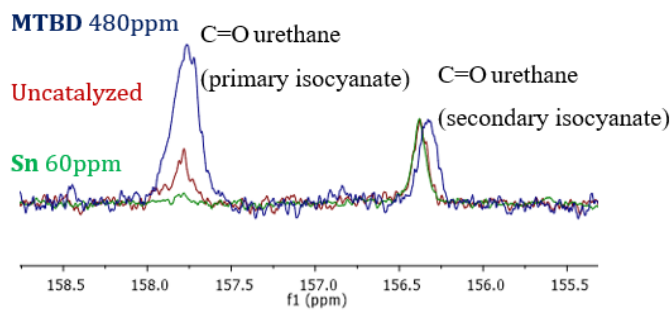


FIGURE 6. Focus on urethane-derived carbonyl chemical shift region of  $^{13}\text{C}$  NMR spectra of NCO-terminated prepolymers in acetone- $d_6$ .

Three different catalyst behaviors are unveiled by  $^{13}\text{C}$  NMR spectroscopy. The first category of catalysts, mainly composed of metallic catalysts, promoted the reactivity of the secondary isocyanate function alike the intrinsic reactivity showcased in the uncatalyzed system ( $S < 1$ , Table 2). Metallic catalysts are hindered by the unfavorable sterics of the primary isocyanate and consequently promote the reactivity of the secondary isocyanate function. Tin catalyst (**Sn**) is identified as the most selective catalyst: 12.5 secondary isocyanate functions reacted for one primary isocyanate. The second category of catalysts, formed by organic catalysts, led to a significant inversion of selectivity in favor of the primary isocyanate function ( $S > 1$ , Table 2). The bicyclic guanidine **MTBD** is the most selective organic catalyst toward the primary isocyanate with a selectivity  $S$  equal to  $\sim 3$ . Metallic catalysts are thus more selective for the secondary isocyanate than organic catalysts are bias for the primary isocyanate. The third category of catalysts, also comprised of organic catalysts, favored the isoreactivity of the two isocyanate functions of IPDI ( $S \sim 1$ , Table 2).

These results suggest that inefficient organic catalysts promote almost isoreactivity (not too far from uncatalyzed system) and only efficient organic catalysts lead to an inversion of selectivity, compared to the inherent bias of the asymmetric IPDI monomer. The mode of action of these organocatalysts, based on nucleophilic and/or basic mechanism,<sup>11</sup> could be less impacted by the steric hindrance of the primary isocyanate. Lomölder *et al.* suggested that DABCO interacted with the secondary isocyanate function which is the most reactive and locked the possibility for polyols to react with it, which could explain the increase of the primary isocyanate reactivity.<sup>19</sup>

TABLE 2. Values of catalyst selectivity toward the primary and the secondary isocyanate functions of IPDI determined by <sup>13</sup>C NMR analyses of NCO-terminated prepolymers.

<b>Catalyst</b>	<b>Catalyst selectivity S (<sup>13</sup>C NMR urethane carbonyl ratio) *</b>
<b>Uncatalyzed</b>	0.68
<b>Sn 60ppm</b>	0.08
<b>Fe 240ppm</b>	0.19
<b>Zn 240ppm</b>	0.22
<b>Ti 70ppm</b>	0.16
<b>Bi 58ppm</b>	0.25
<b>Zr 390ppm</b>	0.33
<b>TBO.HCl 462ppm</b>	0.54
<b>TBD 440ppm</b>	0.84
<b>DBN 495ppm</b>	0.75
<b>DBU 600ppm</b>	1.12
<b>DABCO 450ppm</b>	1.54
<b>MTBO 392ppm</b>	1.83
<b>TMG 2300ppm</b>	1.95
<b>TBO.Na 442ppm</b>	2.32
<b>BTMG 3500ppm</b>	2.32
<b>TBD.Na 375ppm</b>	2.76
<b>MTBD 480ppm</b>	2.98

\* S represents the selectivity of each catalyst and it is determined as the ratio of the integration of the two carbonyl signals, i.e.  $S = (C=O(\text{primary monourethane})) / (C=O(\text{secondary monourethane}))$  using liquid <sup>13</sup>C NMR spectroscopy.

In order to understand the origin of these different selectivities, we conducted mechanistic studies (see SI) using equimolar mixtures at room temperature or 60-80°C of model molecules for IPDI (primary or secondary aliphatic monoisocyanates) and PPG (isopropanol, since terminal -OH moieties are always secondary), and of selected catalysts: **Sn** ( $S_{<<1}$ ), **MTBD** ( $S_{>1}$ ) or **DBU** ( $S_{-1}$ ). In the presence of isopropanol, liquid  $^1\text{H}$  and  $^{13}\text{C}$  NMR spectra only indicated an interaction between the oxygen atom of the alcohol and the metallic center for **Sn** catalyst or the nitrogen atom of the C=N double bond for **MTBD** and **DBU** (Figures S9 to S14, SI). To accurately model IPDI, the primary and secondary isocyanate used were cyclohexyl isocyanate and cyclohexane methyl isocyanate. In the presence of **Sn** catalyst, liquid  $^1\text{H}$  and  $^{13}\text{C}$  NMR spectra indicated a similar interaction of the nitrogen or the oxygen atom of the primary or secondary isocyanate function with the metallic center Sn due to slight shift of some characteristic signal of the isocyanates and the catalyst (C=O bond of **Sn** catalyst, CH/CH<sub>2</sub> group in alpha position of NCO function, Figures S15, S16 and S21 SI). This study suggests that **Sn** catalyst follow a mechanism governed by steric hindrance because the secondary function of IPDI, less hindered, is likely promoted despite liquid NMR spectra failing to display a preferential interaction between the **Sn** catalyst and the primary or secondary isocyanate (they both interact with the metal center). In the case of **MTBD**,  $^1\text{H}$  and  $^{13}\text{C}$  NMR spectra indicated the formation of an adduct of **MTBD** with 2 molecules of primary isocyanate whereas no chemical reaction or interaction occur in presence of the secondary isocyanate (Figures S17, S18, S22, S23 in SI). On the contrary, NMR spectra suggested that **DBU** reacted with the primary and the secondary isocyanate function to form an adduct with one molecule of **DBU** and 2 molecules of isocyanate (Figures S19, S20, S24 and S25 in SI). The formation of these adducts confirms the selectivities of the catalysts determined during the prepolymerization by NMR analysis. In terms of reactivity, Landais *et al.* suggested that the adducts of **MTBD** with benzyl isocyanate were reversible contrary to the adducts of **DBU**, which could explain the low activity of this catalysts during polymerization.<sup>11</sup> During reaction with a high ratio NCO/OH, nucleophilic mechanism, which implies isocyanate and catalyst, could predominate on the basic mechanism and consequently rapidly lead to the deactivation of **DBU** if the formation of adducts are irreversible. In our case and with **MTBD**, the formation of the adduct with aliphatic isocyanate might also be reversible and is clearly not detrimental to the reaction with primary functions.

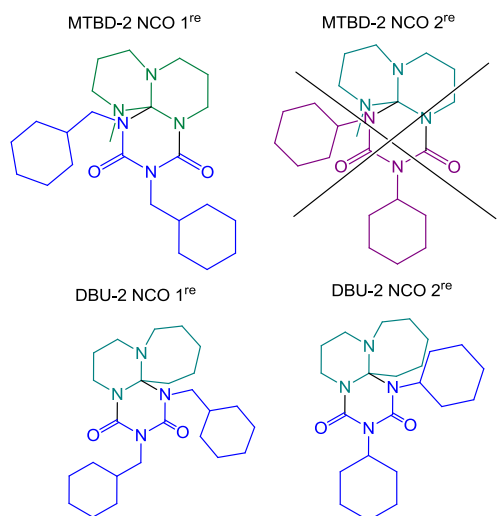


FIGURE 7. Structure of MTBD and DBU adduct with cyclohexanemethyl isocyanate (NCO 1<sup>re</sup>) and cyclohexyl isocyanate (NCO 2<sup>re</sup>).

Crosslinking of NCO-terminated prepolymers in presence of polyester diols and polyether triols.

The crosslinking stage occurred between NCO-terminated prepolymers in the presence of a polyester diol and a polyether triol at a NCO/OH ratio equal to 1.86 at 25°C. This time, air moisture is not avoided, similarly to industrial crosslinking conditions. The presence of urea beside urethane functionalities is actually advantageous for H-bonding-derived properties.<sup>1,3,4,32</sup> Kinetics of crosslinking were determined by FTIR-ATR spectroscopy with samples of thin films of polymers (300  $\mu\text{m}$  thick) realized on glass plates using a film applicator. During crosslinking, the decrease of the NCO stretching band at 2251  $\text{cm}^{-1}$  was monitored in order to represent the consumption of isocyanate functions versus crosslinking time (Figure 8, experimental details are provided in SI Figure S1). As for the prepolymerization kinetics monitoring, FTIR analyses were quasi-quantitative thanks to the homogeneity of the crosslinking medium. At this stage, different combinations of prepolymerization and crosslinking catalysts with similar or opposite selectivities are used in order to identify innovative and effective catalysts combinations to significantly decrease crosslinking time. In this section, Prepolymerization and Crosslinking catalysts are designated as P(catalyst) and C(catalyst).

In the presence of catalysts of prepolymerization and crosslinking with similar selectivities (*i.e.* P(**Zn** 240ppm)/C(**Zn** 240ppm), P(**Sn** 60ppm)/C(**Sn** 60ppm)), nearly 3 weeks are required to obtain the final crosslinked films at 25°C (no more noticeable NCO stretching band on IR spectra). Until around 70% of isocyanate conversion, these two catalytic systems provided a fast rate and then slowed down to reach eventually 100% of isocyanate conversion. On the contrary, combinations that implied catalysts with opposite selectivities at the two stages led to a complete crosslinking in nearly 1 week (*i.e.* P(**Sn** 60ppm)/C(**MTBD** 1200ppm) and P(**Zn** 240ppm)/C(**MTBD** 1200ppm), Figure 8). These associations of



catalysts with opposite selectivities allowed to decrease significantly the time to complete crosslinking (<1 week against 3 weeks for quantitative crosslinking, *i.e.* no NCO residues) and render these polymerization systems industrially viable up to a temperature range of reaction of 40-60°C. Beyond this temperature, the crosslinking kinetics no longer depended on the associations of the catalysts but solely on the temperature (thermodynamic control).

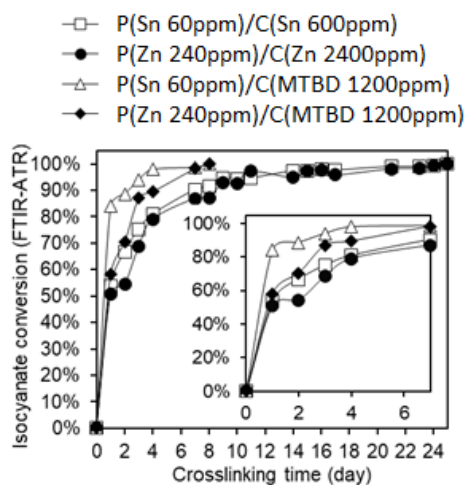


FIGURE 8. Influence of prepolymerization and crosslinking catalysts with various selectivities on crosslinking rate at 25°C, monitored by FTIR-ATR spectroscopy.

These results can once again be explained *via* the selectivity of the chosen catalyst. When **Sn**- or **Zn**-catalysts are used at the prepolymerization stage, secondary monourethane are formed as was determined previously by NMR spectroscopy. At the end of the prepolymerization, primary isocyanate functions will be the remaining reactive groups at the crosslinking stage (Figure 9). In order to improve the crosslinking rate, it is thus necessary to use a catalyst that promotes the reaction of primary isocyanate functions and consequently a crosslinking catalyst with the opposite selectivity to that of the prepolymerization catalyst (Figure 9).

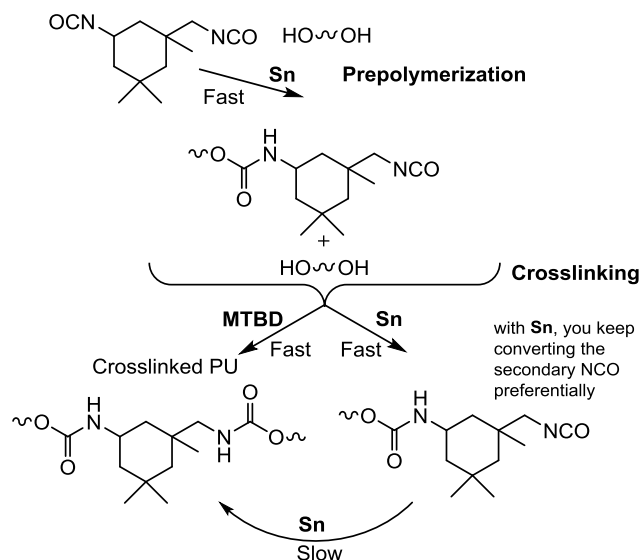


FIGURE 9. Influence of selectivities of catalysts and catalyst combinations on prepolymerization and crosslinking rates.

Harnessing selectivity of catalysts led to the successive and controlled reaction of primary and secondary isocyanate functions during prepolymerization and then at the crosslinking stage (or *vice versa*). To confirm our hypothesis, we resorted to solid-state NMR to monitor *in-situ* the crosslinking of prepolymers in the presence of polyols and air moisture (Figure S26, SI).  $^1\text{H}$  MAS NMR (magic angle spinning) spectra are firstly recorded on NCO-terminated prepolymers (spectra in Figure S27, SI). Polyols are then introduced in rotor (MAS NMR sample holder) already containing the prepolymer medium. The high spinning frequency (rotation at 12.5 kHz) allows fast mixing at the early stage of reaction between remaining NCO and OH moieties and formation of a film along the rotor wall (conditions similar to the study by FTIR-ATR spectroscopy), leading to a convenient *in-situ* monitoring of the crosslinking stage (Figure S26, SI and Figures 9 and 10). Enhanced mobility of our selected PU systems yielded relatively narrow NMR signals for a MAS NMR spectra. Akin to liquid  $^1\text{H}$  and  $^{13}\text{C}$  NMR spectra (Figures S7 and S8 in SI), NCO-terminated prepolymers spectra presented two specific signals of urethane functions resulting from the reaction of the primary or the secondary isocyanate functions with alcohol groups on  $^1\text{H}$  MAS NMR spectra (Figure 10). The influence of two catalytic systems involving catalysts with opposite selectivity are studied, *i.e.* a) P(**Sn** 60ppm)/C(**MTBD** 1200ppm) and b) P(**MTBD** 480ppm)/C(**Sn** 60ppm).

For the catalyst combination a) (*i.e.* P(**Sn** 60ppm)/C(**MTBD** 1200ppm)), one major signal corresponding to the urethane proton NH resulting from the reaction of the secondary isocyanate with alcohol function is observed at the beginning of the crosslinking stage (Figure 10), confirming the reactive bias of the **Sn** catalyst. During the first minutes of crosslinking, the intensity of the signal corresponding to urethane proton NH derived from primary isocyanate significantly increases due to the selective action of the **MTBD** catalyst. These qualitative evolutions of signal intensities during the crosslinking stage within the NMR probe confirmed the successive reactions of the secondary and primary isocyanate functions (or

*vice versa*, see below) in these favorable catalyst combinations. The initial shifts from the red reference representing prepolymers, is due to the overall major change in H-bonding networks brought about by the mixing-in of OH-containing polyols and adventitious moisture (see SI for MAS NMR experimental details). At the end of crosslinking, cylindrical thin films (similar to what is obtained on glass plates) were obtained and could be extracted from the rotors (Figure 10, insert).

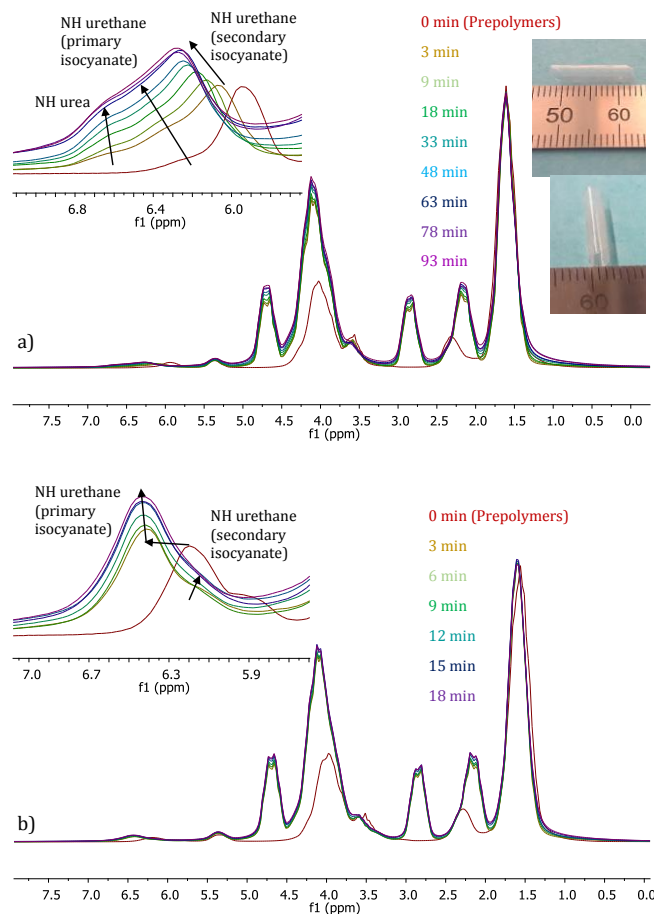


FIGURE 10. <sup>1</sup>H MAS NMR spectra of *in-situ* crosslinking between NCO-terminated prepolymers, polyether triol, polyester diol and air moisture in presence of different catalyst combinations: a) P(Sn 60ppm)/C(MTBD 1200ppm) and b) P(MTBD 480ppm)/C(Sn 60ppm).

Chemical shift between the time  $t_0$  and  $t$  is thus due to the addition of polyols which induced a change of polarity in the medium. A third signal emerged at higher chemical shift and seemed to increase during crosslinking and could be attributed to the formation of urea NH functions. The different environment of the N-H bonds belonging to the different conformations of urethane and urea moieties in the bulk increases the anisotropy of the medium as evidenced by dipolar broadening of the signals, preventing precise quantifications.

The opposite results is observed for the catalyst combination b) P(**MTBD** 480ppm)/C(**Sn** 600ppm) (Figure 10). Deconvolution of the two urethane NH signals is realized in this case and confirmed that the intensity of the NH signal resulting from the reaction of primary isocyanate remained constant during the first minutes of the crosslinking whereas the NH urethane signal corresponding to the reaction of secondary isocyanate significantly increased (Figure S28, SI). These deconvolution remained qualitative due to the anisotropic medium in solid-state NMR. This *in-situ* crosslinking confirmed that harnessing catalyst combinations with opposite selectivities allows to considerably increase reaction kinetics by the successive reaction of the two isocyanate functions of IPDI at the prepolymerization and crosslinking stages. Although no difference are observed on crosslinked-polyurethane microstructures by MAS NMR spectroscopy due to dipolar broadening, seeming to indicate the networks are independent of the choice of catalyst, DSC & DMA analyses revealed that catalyst combinations have a significant impact on the crosslinked polyurethanes thermal and thermomechanical properties (Figures S29-S31 in SI and Table 3). Depending on the choice of catalyst combinations, polyurethane films can reach a range of glass transition temperatures from -34.8°C to -21.1°C (Table 3). Additionally, height, width and integral values of  $\tan \delta$  related to the damping ratio of the material can be tuned by catalysis. Adjusting the thermomechanical properties of PU-based materials could prove invaluable for numerous targeted applications. Overall the combination of MAS NMR spectroscopy with thermomechanical analyses is a powerful methodology for the study of crosslinking to yield intricate and potentially dynamic networks.<sup>33</sup>

TABLE 3. Values of glass transition of crosslinked polyurethane thin films realized at 25°C on glass plate in presence of different catalyst combinations.

Entry	P(catalyst)	C(catalyst)	$T_g$ (°C)	$T_\alpha$ (°C)	Height	Width	Integral
					$\tan \delta$	$\tan \delta$ (°C)	$\tan \delta$ (°C)*
1	<b>Sn</b> 60ppm	<b>Sn</b> 600ppm	-21.1	23.1	0.66	52	42
2	<b>Sn</b> 60ppm	<b>MTBD</b> 1200ppm	-24.2	30.6	0.55	101	55
3	<b>MTBD</b> 480ppm	<b>Sn</b> 600ppm	-22.7	17.9	0.60	60	46
4	<b>MTBD</b> 480ppm	<b>Zn</b> 2400ppm	-32.0	nd**	nd	nd	nd
5	<b>Zn</b> 240ppm	<b>MTBD</b> 1200ppm	-34.8	nd	nd	nd	nd
6	<b>Zn</b> 240ppm	<b>Zn</b> 2400ppm	-25.7	29.4	0.64	84	57

\* Integration of  $\tan \delta$  curve in the temperature range of -70 to 120°C

\*\* nd: not determined for this sample

## CONCLUSION

Polyurethanes based on aliphatic isocyanates such as isophorone diisocyanate can be obtained in presence of selected catalysts *via* a two-stage process (prepolymerization and crosslinking) in order to considerably increase reaction kinetics, and allow for industrial applications relying on coating processes. Tin-free or even metal-free catalysts have been identified to significantly decrease reaction times from 42 hours at 80°C to few hours at the prepolymerization stage without altering prepolymer properties compared to those obtained with standard tin catalyst. Different prepolymer structures have been evidenced by liquid NMR spectroscopy due to the particular selectivity of each catalyst toward the reactivity of either primary or secondary isocyanate functions. Three different catalyst behaviors have been identified by <sup>13</sup>C-NMR spectroscopy. The first category of catalysts, mostly composed of metallic catalysts, favored the reactivity of the secondary isocyanate whereas the second category, exclusively comprised of organic catalysts, promoted the reaction of primary isocyanate with alcohol functions. The third category led to an isoreactivity of the two asymmetric isocyanate functions. These selectivities can be harnessed at the crosslinking stage to significantly decrease reaction time by identifying innovative and judicious catalyst combinations with opposite selectivities. These catalyst combinations led to a controlled and successive reaction of the two isocyanate groups, confirmed by *in-situ* monitoring of the crosslinking stage by solid-state NMR. The switch in catalyst selectivity as a method to efficiently promote crosslinking of IPDI-derived formulations could be evidenced using operando solid-state MAS NMR spectroscopy of polymer crosslinking for the first-time.

Adjusting the selectivity of the chosen catalysts considerably influenced prepolymerization and crosslinking rates but also polyurethanes properties, notably the  $T_g$ . This study also suggests efficient tin-free or even metal-free catalysts for the synthesis of polyurethanes based on an industrially relevant aliphatic diisocyanate monomer. This study finally paves the way towards tailored polyurethane architectures by appropriate choice of catalyst combinations at the different stages of the material elaboration.

## ASSOCIATED CONTENT

### Supporting Information

This material is available free of charge via the Internet at <http://pubs.acs.org>

Materials, Synthesis and characterization procedures. Complementary reaction mechanisms and calculations for kinetics.

Molar masses and viscosities of prepolymers. IR, NMR spectra. DSC, DMA thermograms.

## AUTHOR INFORMATION

## Corresponding Authors

\* Vincent Monteil – CNRS, University of Lyon 1 - CPE Lyon, Villeurbanne, France; E-mail: [vincent.monteil@univ-lyon1.fr](mailto:vincent.monteil@univ-lyon1.fr)

\* Jean Raynaud – CNRS, University of Lyon 1 - CPE Lyon, Villeurbanne, France; E-mail: [jean-raynaud@univ-lyon1.fr](mailto:jean-raynaud@univ-lyon1.fr)

## Author Contributions

The experimental work was realized by PA, with the MAS NMR in collaboration with DG. The manuscript was written through contributions of all authors, and in particular under the guidance of JR and VM.

## Notes

There are no conflicts to declare.

## ACKNOWLEDGMENT

The authors acknowledge Franck Collas for his expertise on thermomechanical analyses and Bostik for financial support (PA's PhD fellowship). Financial support from the IR-RMN-THC FR-3050 CNRS for conducting the research is gratefully acknowledged.

## ABBREVIATIONS

PU, Polyurethane; Sn, Dioctyltin dilaurate; Ti, Diisopropoxybis(ethylacetato)titanate; Zn, Zinc neodecanoate; Bi, Bismuth neodecanoate; Zr, Zirconium(IV) acetylacetonate; Fe, Fer(II) triflate; DABCO, 1,4-diazabicyclo(2.2.2)octane; DBU, 1,8-diazabicyclo(5.4.0)undec-7-ene; DBN, 1,5-diazabicyclo(4.3.0)non-5-ene; TBD, 1,5,7-triazabicyclo(4.4.0)dec-5-ene; MTBD, 7-methyl-1,5,7-triazabicyclo(4.4.0)dec-5-ene; TMG, 1.1.3.3-Tetramethylguanidine; BTMG, 2-tertbutyl-1.1.3.3-Tetramethylguanidine; P(catalyst); prepolymerization catalyst; C(catalyst), crosslinking catalyst.

## REFERENCES

- (1) M. Szycher Ph.D. *Szycher's Handbook of Polyurethanes, Second Edition*, CRC Press **2013**.
- (2) H.-W. Engels, H.-G. Pirkl, R. Albers, R. W. Albach, J. Krause, A. Hoffmann, H. Casselmann, J. Dormish, Polyurethanes: Versatile Materials and Sustainable Problem Solvers for Today's Challenges *Angew. Chem. Int. Ed.* **2013**, *52*, 9422–9441.
- (3) J. Akindoyo, M. Beg, S. Ghazali, M. Islam, N. Jeyaratnam, A. R. Yuvaraj, Polyurethane types, synthesis and applications – a review *RSC Adv.* **2016**, *6*, 114453–114482.
- (4) C. Hepburn, *Polyurethane Elastomers*, Springer Science & Business Media **2012**.

- (5) F. Méchin, 100 ans de Polymères: Les polyuréthanes, "couteau suisse" des matériaux polymères. *Actual. Chim.* **2020-2021**, 456-457-458, 53-63.
- (6) M. Ionescu, *Chemistry and Technology of Polyols for Polyurethanes*, Rapra Technology Limited **2005**.
- (7) A. Farkas, G. A. Mills, in *Adv. Catal.* (Eds.: D.D. Eley, P.W. Selwood, P.B. Weisz, A.A. Balandin, J.H. De Boer, P.J. Debye, P.H. Emmett, J. Horiuti, W. Jost, G. Natta, E.K. Rideal, H.S. Taylor), Academic Press **1962**, 393-446.
- (8) H. Sardon, A. Pascual, D. Mecerreyes, D. Taton, H. Cramail, J. L. Hedrick, Synthesis of Polyurethanes Using Organocatalysis: A Perspective *Macromolecules* **2015**, *48*, 3153-3165.
- (9) H. Sardon, L. Irusta, M. J. Fernandez-Berridi, Synthesis of isophorone diisocyanate (IPDI) based waterborne polyurethanes: Comparison between zirconium and tin catalysts in the polymerization process. *Prog. Org. Coat.* **2009**, *66*, 291-295.
- (10) H. Sardon, A. C. Engler, J. M. W. Chan, J. M. García, D. J. Coady, A. Pascual, D. Mecerreyes, G. O. Jones, J. E. Rice, H. W. Horn, J. L. Hedrick, Organic Acid-Catalyzed Polyurethane Formation via a Dual-Activated Mechanism: Unexpected Preference of N-Activation over O-Activation of Isocyanates. *J. Am. Chem. Soc.* **2013**, *135*, 16235-16241.
- (11) J. Alsarraf, Y. A. Ammar, F. Robert, E. Cloutet, H. Cramail, Y. Landais, Cyclic Guanidines as Efficient Organocatalysts for the Synthesis of Polyurethanes. *Macromolecules* **2012**, *45*, 2249-2256.
- (12) F.-Z. Belmokaddem, J. Dagonneau, J. Lhomme, R. Blanc, A. Garduno-Alva, C. Maliverney, A. Baceiredo, E. Maerten, E. Fleury, F. Méchin, Novel nucleophilic/basic and acidic organocatalysts for reaction between poorly reactive diisocyanate and diols. *Designed Monomers & Polymers* **2016**, *19*, 347-360.
- (13) Y. Schellekens, B. V. Trimpont, P.-J. Goelen, K. Binnemans, M. Smet, M.-A. Persoons, D. D. Vos, Tin-free catalysts for the production of aliphatic thermoplastic polyurethanes. *Green Chem.* **2014**, *16*, 4401-4407.
- (14) V. de Lima, N. da Silva Pelissoli, J. Dullius, R. Ligabue, S. Einloft, Kinetic study of polyurethane synthesis using different catalytic systems of Fe, Cu, Sn, and Cr. *J. Appl. Polym. Sci.* **2010**, *115*, 1797-1802.
- (15) P. Arnould, L. Bosco, F. Sanz, F. N. Simon, S. Fouquay, G. Michaud, J. Raynaud, V. Monteil, Identifying competitive tin- or metal-free catalyst combinations to tailor polyurethane prepolymer and network properties. *Polym. Chem.* **2020**, *11*, 5725-5734.
- (16) F. Sanz, G. Michaud, F. Simon, J. Raynaud, V. Monteil, L. Bosco, *Method for Producing a Composition Comprising a Polyurethane with Nco End Groups*, **2017**, WO2019122706A1.
- (17) A. V. Cunliffe, A. Davis, M. Farey, J. Wright, The kinetics of the reaction of isophorone diisocyanate with monoalcohols. *Polymer.* **1985**, *26*, 301-306.

- (18) K. Hatada, K. Ute, S. Peter Pappas, E,Z assignments of isophorone diisocyanate (IPDI) and their implications on the relative reactivity of the isocyanate groups. *J. Polym. Sci. Part C Polym. Lett.* **1987**, *25*, 477–480.
- (19) R. Lomölder, F. Plogmann, P. Speier, Selectivity of isophorone diisocyanate in the urethane reaction influence of temperature, catalysis, and reaction partners. *J. Coat. Technol.* **1997**, *69*, 51–57.
- (20) O. Lorenz, H. Decker, G. Rose, NCO-prepolymers of diisocyanates containing different reactive NCO groups. *Angew. Makromol. Chem.* **1984**, *122*, 83–99.
- (21) J.-F. Gerard, P. L. Percec, Q. T. Pham, Polyuréthanes à propriétés émulsifiantes et électrolytiques, 2. Cinétique de polycondensation en solution des alkylimino-2,2' diéthanols avec le diisocyanate d'isophorone. Etude par <sup>1</sup>H et <sup>13</sup>C NMR. *Makromol. Chem.* **1988**, *189*, 1719–1737.
- (22) N. Bialas, H. Höcker, M. Marschner, W. Ritter, <sup>13</sup>C NMR studies on the relative reactivity of isocyanate groups of isophorone diisocyanate isomers. *Makromol. Chem.* **1990**, *191*, 1843–1852.
- (23) K. Hatada, K. Ute, K.-I. Oka, S. P. Pappas, Unambiguous <sup>13</sup>C-NMR assignments for isocyanate carbons of isophorone diisocyanate and reactivity of isocyanate groups in Z - and E-stereoisomers. *J. Polym. Sci. Part A Polym. Chem.* **1990**, *28*, 3019–3027.
- (24) M. Rochery, I. Vroman, T. M. Lam, Kinetic model for the Reaction of IPDI and Macrodiols: Study on the relative Reactivity of Isocyanate groups. *J. Macromol. Sci. Part A* **2000**, *37*, 259–275.
- (25) A. Prabhakar, D. K. Chattopadhyay, B. Jagadeesh, K. V. S. N. Raju, Structural investigations of polypropylene glycol (PPG) and isophorone diisocyanate (IPDI)-based polyurethane prepolymer by 1D and 2D NMR spectroscopy. *J. Polym. Sci. Part A Polym. Chem.* **2005**, *43*, 1196–1209.
- (26) H.-K. Ono, F. N. Jones, S. P. Pappas, Relative reactivity of isocyanate groups of isophorone diisocyanate. Unexpected high reactivity of the secondary isocyanate group. *J. Polym. Sci. Part C Polym. Lett.* **1985**, *23*, 509–515.
- (27) D. K. Chattopadhyay, N. Prasada Raju, M. Vairamani, K. V. S. N. Raju, Structural investigations of polypropylene glycol (PPG) and isophorone diisocyanate (IPDI) based polyurethane prepolymer by matrix-assisted laser desorption/ionization time-of-flight (MALDI-TOF)-mass spectrometry. *Prog. Org. Coat.* **2008**, *62*, 117–122.
- (28) S. Lee, J. H. Choi, I.-K. Hong, J. W. Lee, Curing behavior of polyurethane as a binder for polymer-bonded explosives. *J. Ind. Eng. Chem.* **2015**, *21*, 980–985.
- (29) K. Hailu, W. Becker, A. Bendfeld, E. Geissler, In-situ characterization of the cure reaction of HTPB and IPDI by simultaneous NMR and IR measurements. *Polym. Test.* **2010**, *29*, 513–519.
- (30) W. Wu, X. Zeng, H. Li, X. Lai, Z. Yan, Synthesis and characterization of polyhydroxylated polybutadiene binding 2,2'-thiobis(4-methyl-6-tert-butylphenol) with isophorone diisocyanate. *J. Appl. Polym. Sci.* **2014**, *131*, 40942.



- (31) N. von Wolff, C. Villiers, P. Thuéry, G. Lefèvre, M. Ephritikhine, T. Cantat, Reactivity and Structural Diversity in the Reaction of Guanidine 1,5,7-Triazabicyclo(4.4.0)dec-5-ene with CO<sub>2</sub>, CS<sub>2</sub>, and Other Heterocumulenes. *Eur. J. Org. Chem.* **2017**, 676–686.
- (32) I. Yilgör, E. Yilgör, G. L. Wilkes, Critical parameters in designing segmented polyurethanes and their effect on morphology and properties: A comprehensive review. *Polymer* **2015**, 58, A1–A36.
- (33) J. L. Swartz, D. T. Sheppard, G. Haugstad, W. R. Dichtel, Blending Polyurethane Thermosets Using Dynamic Urethane Exchange. *Macromolecules* **2021**, 54, 11126–11133.